Outage Performance of Satellite Terrestrial Full-Duplex Relaying Networks with Co-Channel Interference

Tan N. Nguyen, *Member, IEEE*, Lam-Thanh Tu, Dinh-Hieu Tran, Van-Duc Phan, Miroslav Voznak, *Senior Member, IEEE*, Symeon Chatzinotas, *Senior Member, IEEE*, Zhiguo Ding, *Fellow, IEEE*

***Abstract*—This letter investigates the performance of the satellite-terrestrial networks (STN), where a satellite tries to transmit information to a ground user through the help of multiple decode-and-forward relays and the existence of co-channel interference sources. In particular, the full-duplex technique and partial relay selection are applied at the relay to increase the total throughput at the destination, enhance the system reliability, and reduce the complexity. In this context, the outage probability (OP) is computed in a closed-form expression. Numerical results are provided to confirm the accuracy of the proposed mathematical framework. Our findings illustrate that the outage performance can be effectively enhanced by increasing either number of relays or transmit power.**

***Index Terms*—Co-channel interference, full-duplex, outage probability, satellite-terrestrial networks, shadowed-rician fading,**

I. Introduction

Satellite communications has been recognized by the third generation partnership project (3GPP) as a complementary solution to the 5G-Advanced system towards the sixth generation (6G) networks owing to supporting a wide range of terminals, low manufacturing cost, size, and weight [1]. However, the performance of mobile satellite systems is constrained by the masking effect caused by obstacles that block the line-of-sight (LoS) link between terrestrial users and the satellite. Additionally, the situation is significantly escalated in case of low satellite elevation angles and/or indoor users. As a result, the satellite-terrestrial networks (STN) has emerged as a promising solution to overcome such issues [2]. In the STN system, ground terminals receive signals from the satellite with the help of fixed or mobile relays.

The performance of the STN was investigated in [2]–[10]. Authors in [3] addressed the ergodic capacity of the asymmetric free-space optical (FSO)/radio frequency (RF) satellite-unmanned aerial vehicle (UAV)-terrestrial networks in the closed-form expression. However, they focused on the combination of FSO and RF links rather than employing merely the RF link. Similarly, the ergodic sum rate of the uplink non-orthogonal multiple access (NOMA) of the satellite-aerial-ground networks was addressed in [4], [5]. However, they derived the ergodic capacity instead of studying the outage probability (OP). Sharma *et. al.* in [7], on the other hand, investigated the OP of the cognitive STN. Nonetheless, they studied the cognitive radio networks while this letter simply addresses the performance of the STN. The impact of the imperfect channel state information (CSI) on the OP performance of the STN was studied in [8], [9]. The results in [8] illustrate that by increasing the number of relays, the OP can be enhanced 10-times and can overcome the impact of the imperfect CSI. These works, nonetheless, ignored the influences of co-channel interference (CCI). The authors of [10] derived the OP under the multi-user and multi-relay STN systems. However, for each transmission, only one relay was involved to help the source and destination transmission. Additionally, they also did not consider the impact of the CCI and full-duplex (FD) relaying at the relay. The relay selection in STN was studied in [2]. Particularly, the authors in [2] investigated the performance of the CST system under a complicated relay selection that requires extensive feedback information and high computation at the destination. Specifically, in order to select the best relay to assist the transmission from source to destination, [2] requires perfect global channel state information (CSI) from source to relays, from relays to destination, and from all interferer to relays and destination. The adopted relay selection, on the other hand, is simpler and effective since it solely requires the channel gain from S to relays as like [11]. However, different from [11] the present work takes into account the impact of the CCI as well as FD relaying while the work in [11] ignored it.

In contrast to the above-mentioned works that only investigated the integration between satellite and FD or satellite and CCI, we investigate the performance of the STN system by jointly considering the influences of CCI and FD relaying, which is highly challenging and not studied in the literature. The main contributions and novelties of this work can be summarized as follows:

- To the best of our knowledge, this is the first work to analyze the performance of a STN while incorporating FD and CCI.
- Partial relay selection is adopted to both enhance the system reliability and reduce the complexity.

Manuscript received Jan. 16th, 2021; revised Apr. 20th, 2022; accepted May 08th, 2022; this work is supported in part by the Van Lang University, Vietnam and by the Ministry of Education, Youth and Sport of the Czech Republic under the grant SP2021/25 conducted at the VSB – Technical University of Ostrava. Corresponding author: *Van-Duc Phan*, (email: duc.pv@vlu.edu.vn). The associate editor coordinating the review of this article and approving it for publication was Dr. Nasir Saeed.

Tan N. Nguyen and Lam-Thanh Tu are with the Communication and Signal Processing Research Group, Faculty of Electrical and Electronics Engineering, Ton Duc Thang University, Ho Chi Minh City, Vietnam. (e-mail: {nguyennhattan, tulamthanh}@tdtu.edu.vn).

D. H. Tran and S. Chatzinotas are with the Interdisciplinary Centre for Security, Reliability and Trust (SnT), the University of Luxembourg, Luxembourg. (e-mail: {hieu.tran-dinh, symeon.chatzinotas}@uni.lu).

Van-Duc Phan is with Faculty of Automobile Technology, Van Lang University, Ho Chi Minh City, Vietnam, (email: duc.pv@vlu.edu.vn).

Miroslav Voznak is with VSB – Technical University of Ostrava, 70800 Ostrava, Czech Republic. (e-mail: miroslav.voznak@vsb.cz).

Z. Ding is with the School of Electrical and Electronic Engineering, The University of Manchester, Manchester M139PL, United Kingdom (e-mail: zhiguo.ding@manchester.ac.uk).

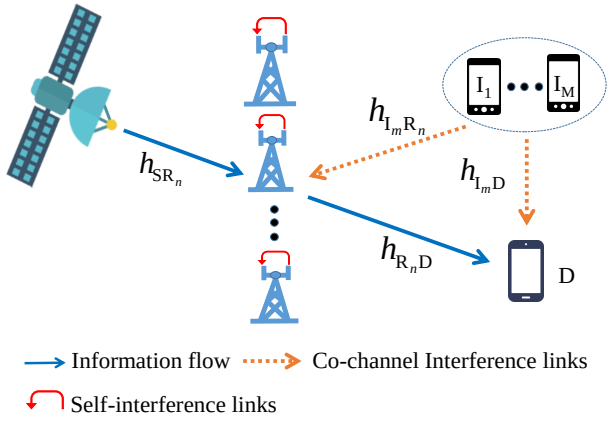

Fig. 1: System model

- The outage probability of end-2-end (e2e) signal-to-interference-plus-noise ratios (SINR) at the receiver is computed in the closed-form expression.
- The impact of the channel gains from the interferer and the relay to the destination are derived based on the mathematical framework.
- Numerical results are given to verify the accuracy of the proposed framework and to compare with the state-of-the-art.

The rest of the paper is organized as follows. The system model is given in Section II. The derivation of key performance metric is presented in Section III. Numerical results are shown in Section IV. Section V concludes the paper.

II. System Model

Let us consider a satellite-terrestrial system comprises of one source node (satellite) denoted by S, an end-device denoted by D and N relays denoted by R_n, $n \in \{1,\ldots,N\}$ under the impact of M interferers denoted by I_m, $m \in \{1,\ldots,M\}$ as shown in Fig. 1. It is noted that satellite and end-device are only equipped with one antenna while relays are equipped with two antennae. There is no direct link from the satellite to the destination[1]. Particularly, the satellite sends information to the mobile user with the help of relay nodes.

A. Channel modelling

In the present paper, we assume that the channel coefficient of the terrestrial links denote as h_{XY}, $X \in \{R_n, I_m\}$ and $Y \in \{R_n, D\}$, follows by Rayleigh fading. Consequently, the channel gain is followed by an exponential distribution with parameters λ_{XY}[2]. Regarding the satellite-terrestrial links, let us consider an arbitrary link from S to the n-th relay denoted by h_{SR_n} the Shadowed-Rician distribution is adopted owing to its high accuracy and lower computation burden compared to other modelling [10]. The probability density function (PDF) of the channel gain (denoted by $\gamma_{\mathrm{SR}_n} = |h_{\mathrm{SR}_n}|^2$) is given as [2], [10]:

$$f_{\gamma_{\mathrm{SR}_n}}(x) = \alpha_n \sum_{k=0}^{m_n-1} \zeta_n(k) x^k \exp\left(-\left(\beta_n - \delta_n\right) x\right), \forall n, \quad (1)$$

where $\alpha_n = \beta_n \left(\frac{2b_n m_n}{2b_n m_n + \Omega_n}\right)^{m_n}$, $\beta_n = \frac{1}{2b_n}$, $\delta_n = \frac{\beta_n \Omega_n}{2b_n m_n + \Omega_n}$ and $\zeta_n(k) = (-1)^k (1-m_n)_k \delta_n^k / (k!)^2$; Ω_n and $2b_n$ are the average power of the LoS and multipath components of the γ_{SR_n}, respectively. Herein, $m_n \in \mathbb{N}$ is the fading severity of γ_{SR_n} and $(x)_k = \prod_{n=0}^{k-1}(x-n)$ is the Pochhammer symbol [15, p. xliii]. With the assistance of [15, eq. 3.351.1], the cumulative distribution function (CDF) of γ_{SR_n} is given as

$$F_{\gamma_{\mathrm{SR}_n}}(x) = 1 - \alpha_n \sum_{k=0}^{m_n-1} \sum_{p=0}^{k} \frac{(-1)^k (1-m_n)_k \delta_n^k}{k!p!\left(\beta_n - \delta_n\right)^{(k+1-p)}} \times x^p \exp\left(-\left(\beta_n - \delta_n\right) x\right). \quad (2)$$

Additionally, we assume that the channel coefficients remain constant during one transmission block and change independently across different transmission blocks.

B. Information transmission

The whole communication takes place in two hops and without the presence of a direct link. More precisely, in the first hop, the satellite broadcasts its information to relays. The selected relay will decode-and-forward[3] (DF) the satellite's signal to the destination in the second hop. Compared with the full relay selection or the highly complicated scheme in [2], the considered one is simpler as it does not require full CSI of the second hop [11]. Additionally, it should be noted that the whole transmission solely takes place in one time-slot since all relays operate in the full-duplex mode, e.g., each relay equips with two antennae that are isolated from each other. The received signal at the best relay denoted by R_a ($R_a : \underset{n\in\{1,\ldots,N\}}{\arg\max}\{\gamma_{\mathrm{SR}_n}\}$) and the destination is then formulated as

$$y_{\mathrm{R}_a} = \sqrt{P_{\mathrm{S}}} h_{\mathrm{SR}_a} x_{\mathrm{S}} + \sqrt{P_{\mathrm{R}_a}} f_a x_{\mathrm{R}_a} + \sum_{m=1}^{M} \sqrt{P_{\mathrm{I}_m}} h_{\mathrm{I}_m\mathrm{R}_a} x_{\mathrm{I}_m} + n_{\mathrm{R}_a}, \quad (3)$$

$$y_{\mathrm{D}} = \sqrt{P_{\mathrm{R}_a}} h_{\mathrm{R}_a\mathrm{D}} x_{\mathrm{R}_a} + \sum_{m=1}^{M} \sqrt{P_{\mathrm{I}_m}} h_{\mathrm{I}_m\mathrm{D}} x_{\mathrm{I}_m} + n_{\mathrm{D}}, \quad (4)$$

where x_{S}, x_{I_m} and x_{R_a} are the transmit signal of the satellite, the m-th interferer and the best relay with $\mathbb{E}\left\{|x_{\mathrm{S}}|^2\right\} = \mathbb{E}\left\{|x_{\mathrm{I}_m}|^2\right\} = \mathbb{E}\left\{|x_{\mathrm{R}_a}|^2\right\} = 1$; $\mathbb{E}\{\bullet\}$ denotes the expectation operator; n_{R_a} and n_{D} are the additive white Gaussian noise (AWGN) with zero mean and N_0 variance. Additionally, due to the imperfection hardware, i.e., phase noise, non-linearity of power amplifier, the self interference (SI) can not be perfectly suppressed thus, there is the residual self-interference (RSI) at all relay nodes. The RSI at the best relay, R_a, denotes as f_a. Besides, P_{S}, $P_{\mathrm{R}_n} = P_{\mathrm{R}}, \forall n$, and $P_{\mathrm{I}_m} = P_{\mathrm{I}}, \forall m$ are the transmit power of the satellite, relays and interference sources, respectively.

From (3) and (4), the SINR at the best relay and the destination can be expressed as follows:

$$\gamma_{\mathrm{R}_a} = \frac{\gamma_{\mathrm{SR}_a}\Psi}{\gamma_{\mathrm{R}_a\mathrm{R}_a}\Phi + \Theta\gamma_{\mathrm{IR}_a} + 1}, \ \gamma_{\mathrm{D}} = \frac{\Phi\gamma_{\mathrm{R}_a\mathrm{D}}}{\Theta\gamma_{\mathrm{ID}} + 1}, \quad (5)$$

[1] An illustrative practical scenario of the considered networks is that a satellite provides mobile streaming services and/or Internet to indoor handheld devices with the help of the terrestrial networks [12], [13].

[2] λ_{XY} can be considered large-scale path-loss [14].

[3] Compared with other popular relaying protocols, i.e., amplify-and-forward (AF) and selective DF protocols, the used DF protocol is adopted because it can realize both the cost-effective and high-performance [3], [16].

where $\Psi = P_{\rm S}/N_0, \Phi = P_{\rm R}/N_0$, $\Theta = P_{\rm I}/N_0$, $\gamma_{{\rm IR}_a} = \sum_{m=1}^{M} |h_{I_m{\rm R}_a}|^2, \gamma_{\rm ID} = \sum_{m=1}^{M} |h_{I_m{\rm D}}|^2$ and $\gamma_{{\rm R}_a{\rm R}_a} = |f_a|^2$. Looking at (5), we observe that the received signals at the relay are subjected to not only CCI but also SI while the destination only experiences the aggregate interference from the M interferer. As DF protocol is employed, the e2e SINR at the destination is then formulated as

$$\gamma_{\rm e2e} = \min\left\{\gamma_{{\rm R}_a}, \gamma_{\rm D}\right\}. \tag{6}$$

In the following, two useful Theorems are introduced in order to compute the important metric, i.e., outage probability, of the considered system model.

Theorem 1: Given a set of N independent and identically distributed (i.i.d.) random variables (RVs), e.g., $X_1, \ldots, X_N$, follows by squared shadowed-Rician distribution with the triple set parameters (m, b, Ω), the CDF of the maximal RV, i.e., $Y = \max\{X_1, \ldots, X_N\}$, is given as follows:

$$F_Y(x) = 1 + \sum_{n=1}^{N} \frac{(-1)^n {\rm T}(n, N, m, \alpha, \beta, \delta)}{n!} x^{p_{\rm S}} \exp\left(-x v_{\rm S}\right), \tag{7}$$

where ${\rm T}(n, N, m, \alpha, \beta, \delta) = \underbrace{\sum_{n_1=1}^{N} \cdots \sum_{n_n=1}^{N}}_{n_1 \neq n_2 \ldots \neq n_n} \times$

$$\sum_{k_1=0}^{m_{n_1}-1} \sum_{p_1=0}^{k_1} \cdots \sum_{k_n=0}^{m_{n_n}-1} \sum_{p_n=0}^{k_n} \prod_{t=1}^{n} \frac{\alpha_{n_t} (-1)^{k_t} \left(1-m_{n_t}\right)_{k_t} \left(\delta_{n_t}\right)^{k_t}}{k_t! p_t! \left(\beta_{n_t} - \delta_{n_t}\right)^{(k_t+1-p_t)}},$$

$v_{\rm S} = \sum_{t=1}^{n} (\beta_{n_t} - \delta_{n_t})$, and $p_{\rm S} = \sum_{t=1}^{n} p_t$.

Proof: The proof is given in Appendix A. ∎

Theorem 2: Given a set of M i.i.d. exponential RVs with parameter λ, the CDF and PDF of the sum of M i.i.d. exponential RVs, i.e., $Y = \sum_{m=1}^{M} X_m$ are then computed as

$$F_Y(y) = \frac{\gamma(M, \lambda y)}{\Gamma(M)}, f_Y(y) = \frac{\lambda^M y^{M-1}}{\Gamma(M)} \exp(-\lambda y). \tag{8}$$

Here $\gamma(\bullet, \bullet)$ is the lower incomplete Gamma function [15, 8.350.1] and $\Gamma(\bullet)$ is the Gamma function [15, 8.310.1].

Proof: The proof is given in Appendix B. ∎

III. Outage Probability Analysis

In this section, we derive the outage probability of the considered system. The OP is referred to the probability that the $\gamma_{\rm e2e}$ is below a predefined threshold. Mathematical speaking, it is formulated as

$$\begin{aligned} {\rm OP} &= \Pr\left(\gamma_{\rm e2e} < \gamma_{\rm th}\right) = \Pr\left(\min\left(\gamma_{{\rm R}_a}, \gamma_{\rm D}\right) < \gamma_{\rm th}\right) \\ &= \Pr\left(\min\left(\frac{\gamma_{{\rm SR}_a}\Psi}{\gamma_{{\rm R}_a{\rm R}_a}\Phi + \Theta\gamma_{{\rm IR}_a} + 1}, \frac{\Phi\gamma_{{\rm R}_a{\rm D}}}{\Theta\gamma_{\rm ID} + 1}\right) < \gamma_{\rm th}\right) \\ &= 1 - \Upsilon_1 \Upsilon_2 \end{aligned} \tag{9}$$

$$\Upsilon_1 = 1 - \int_0^{\infty} \underbrace{\Pr\left(\frac{\gamma_{{\rm SR}_a}\Psi}{\gamma_{{\rm R}_a{\rm R}_a}\Phi + \Theta x + 1} < \gamma_{\rm th}\right)}_{\tilde{\Upsilon}_1(x)} f_{\gamma_{{\rm IR}_a}}(x) dx \tag{10}$$

$$\begin{aligned} \Upsilon_2 &= 1 - \int_0^{\infty} F_{\gamma_{{\rm R}_a{\rm D}}}\left(\frac{\gamma_{\rm th}\left[\Theta x + 1\right]}{\Phi}\right) f_{\gamma_{\rm ID}}(x) dx \\ &= \left(1 + \frac{\lambda_{\rm RD}\gamma_{\rm th}\Theta}{\lambda_{\rm ID}\Phi}\right)^{-M} \exp\left(-\frac{\lambda_{\rm RD}\gamma_{\rm th}}{\Phi}\right), \end{aligned} \tag{11}$$

where $\gamma_{\rm th} = 2^{C_{\rm th}} - 1$ is the targeted rate[4]. $\widetilde{\Upsilon}_1$ in (10) is calculated as

$$\begin{aligned} \widetilde{\Upsilon}_1(x) &= \int_0^{\infty} F_{\gamma_{{\rm SR}_a}}\left(\frac{\gamma_{\rm th}\left[y\Phi + \Theta x + 1\right]}{\Psi}\right) f_{\gamma_{{\rm R}_a{\rm R}_a}}(y) dy \\ &\overset{(a)}{=} 1 + \sum_{n=1}^{N} \frac{(-1)^n {\rm T}(n, N, m, \alpha, \beta, \delta) \lambda_{\rm RR}}{n!} (\gamma_{th}\Phi/\Psi)^{p_{\rm S}} \\ &\times \exp\left(-v_S\gamma_{th}\left[\Theta x + \lambda_{\rm RR}/\Phi\right]/\Psi\right) \\ &\times \sum_{o=0}^{p_{\rm S}} \binom{p_{\rm S}}{o} \left(\frac{\Theta x}{\Phi}\right)^{o} (v_2)^{-v_1(p_{\rm S}, o)} \Gamma\left(v_1(p_{\rm S}, o), v_2/\Phi\right), \end{aligned} \tag{12}$$

where $v_1(p_{\rm S}, o) = p_{\rm S} - o + 1; v_2 = v_S\gamma_{th}\Phi/\Psi + \lambda_{\rm RR}$, $\Gamma(\bullet, \bullet)$ is the upper incomplete Gamma function; (a) is held by employing Theorem 1, the binomial theorem and [15, 3.382.4]. Next, by substituting (12) into (10) and applying [15, 3.381.4], Υ_1 is computed in (13) at the top of the next page where ${\rm N}(\lambda_{\rm RR}, \Phi, v_1, v_2) = \lambda_{\rm RR} \exp(\lambda_{\rm RR}/\Phi) (v_2)^{-v_1(p_{\rm S}, o)} \Gamma(v_1(p_{\rm S}, o), v_2/\Phi)$. Having obtained Υ_1 and Υ_2, the OP of the e2e SINR is then computed in (9).

Proposition 1: OP is a monotonically increasing function with respect to $\lambda_{\rm ID}$ and is a decrease function regarding $\lambda_{\rm RD}$.

Proof: The proof is directly obtained by taking the first-order derivative of OP with respect to $\lambda_{\rm ID}$ and $\lambda_{\rm RD}$, respectively. ∎

Remark 1: Direct inspection Eqs. (9), (11), and (13), we can draw the following insights: i) the OP is computed in closed-form expression without the infinite series as those typical result in the literature; ii) the impact of the SI at relay is dominated by the term ${\rm N}(\lambda_{\rm RR}, \Phi, v_1, v_2)$ while the impact of the CCI is: $(1 + \lambda_{\rm RD}\gamma_{th}\Theta/(\lambda_{\rm ID}\Phi))^{-M}$ and $(\lambda_{\rm IR})^M/(v_3)^{o+M}$.

IV. Numerical Results

In this section, numerical results are presented to verify the accuracy of the proposed mathematical framework as well as to figure out the behaviors of the OP with respect to some important parameters. Without loss of generality, following setup is employed throughout this section: $C_{\rm th}$ = 1.25 bps/Hz, $M = 2$, Ψ = 15 dB, $\lambda_{\rm IR} = \lambda_{\rm ID} = \lambda_{\rm RR} = 5$, and $\lambda_{\rm RD} = 0.2$. The triplet set of heavy shadowing (HS) is (m = 1, b = 0.0635 and Ω = 0.0007) and the average shadowing (AS) is (m = 5, b = 0.3, and Ω=0.279), respectively. All simulation results are produced via Monte-Carlo simulations with 10^6 realizations.

Fig. 2 investigates the impact of Ψ on the performance of the OP. Ψ is considered the average signal-to-noise ratio of the satellite signals. It is to measure the strength of the satellite signal relative to background noise on average. Since Ψ measures the strength of the expected signal versus the unwanted signal, as a result, increasing Ψ monotonically increases in the desired signals, thus, improving the OP. We also observe that the proposed mathematical framework matches perfectly with the computer-based simulation results. Additionally, the OP starts decreasing and reaching the lower

[4] $C_{\rm th}$ is the expected rate that can be considered the minimal required quality-of-service (QoS) that needs to be satisfied in order to avoid an outage event.

$$\Upsilon_1 = \sum_{n=1}^{N} \sum_{o=0}^{p_S} \binom{p_S}{o} \frac{(-1)^{n+1} \mathrm{T}(n, N, m, \alpha, \beta, \delta)}{n!} \left(\frac{\gamma_{th}\Phi}{\Psi}\right)^{p_S} \left(\frac{\Theta}{\Phi}\right)^{o} \mathrm{N}(\lambda_{\mathrm{RR}}, \Phi, v_1, v_2) \frac{\Gamma(o+M)}{\Gamma(M)} \frac{(\lambda_{\mathrm{IR}})^M}{(v_3)^{o+M}}, \quad (13)$$

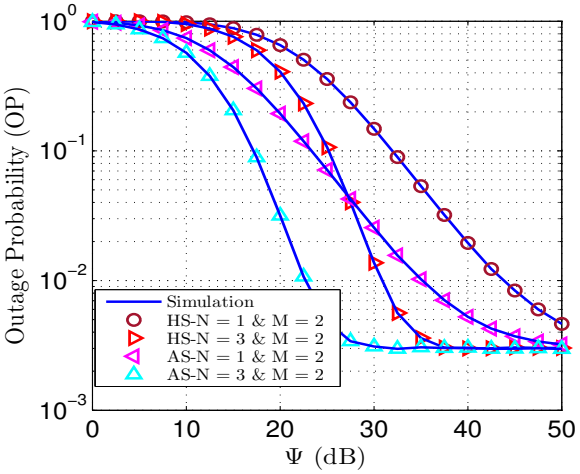

Fig. 2: OP versus Ψ with C_{th} = 1 bps/Hz, Φ = 20 dB and Θ = 1 dB under both heavy shadowing (HS) and average shadowing (AS);

bound when Ψ keeps increasing. The main reason behind this phenomenon is that the γ_{e2e} is constrained by the second hop from R_a to D when $\Psi \gg 1$ that is independent of the Ψ. Additionally, it is interesting to point out that all curves are convergent to a lower bound regardless of the number of relays. However, the larger the number of relays the sooner the convergence to the lower bound. Furthermore, it is evident that the OP's performance under heavy shadowing (denoted by HS) underperforms the average shadowing (denoted by AS). Particularly, under a single relay scenario, i.e., $N = 1$ and $\Psi = 20$ dB, the OP under heavy shadowing is under 0.65 while the OP under the average shadowing is approximately 0.19.

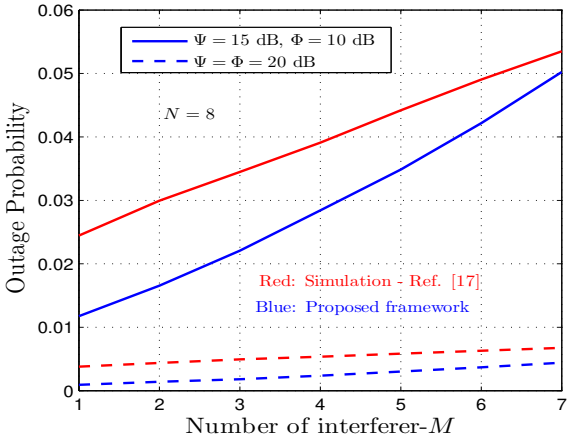

Fig. 3: OP versus M with various value of Φ and Ψ under average shadowing; C_{th} = 1 and Θ = 1 dB.

Fig. 3 stretches the behaviors of the OP with respect to the number of interferers M under various setups of Ψ and Φ. It can be observed that increasing M will degrade the OP's

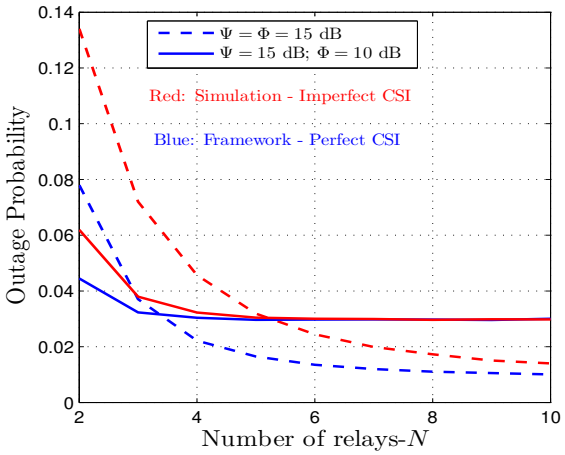

Fig. 4: OP versus N with various value of Ψ and Φ under the average shadowing setup; C_{th} = 1 bps/Hz, M = 2, and Θ = 1 dB. The blue curves are plotted by employing Eq. (9).

performance. The figure also compares the performance of the proposed framework with the work in [17]. Specifically, the red curves that simulate [17] are plotted by employing Monte-Carlo simulations while the blue ones are drawn by Eq. (9). We observe that despite experiencing more interference at the relay owing to FD relaying, the proposed solution always outperforms [17] thanks to the help of multiple relays. This figure also unveils a simple but effective solution to overcome the impact of CCI which is to increase the transmit power at S and/or D.

Fig. 4 unveils the performance of the OP as a function of the number of relays under both perfect and imperfect CSI. Particularly, the following outdated CSI modelling is considered. All channel coefficients from S to R_n, D and from R_n to D are assumed to be imperfect and is modelled as [18]: $\widetilde{h}_{ij} = \rho h_{ij} + \sqrt{1-\rho^2} w_{ij}$, $i \in \{S, R_n\}$, $j \in \{R_n, D\}$, and $n \in \{1, \ldots, N\}$ where $\widetilde{h}_{ij}$ is the outdated version of h_{ij} while $w_{i,j}$ is a complex Gaussian RV with zero mean and the same variance as h_{ij}. It is noted that $w_{i,j}$ is independent of $\widetilde{h}_{ij}$. $\rho \in [0, 1]$ is the correlation coefficient and is calculated by $J_0(2\pi f_d \tau)$, where $J_0(.)$ is the zeroth-order Bessel function of the first kind, f_d kHz is the Doppler shift and τ is the feedback delay. According to [19], we choose $f_d = 1.9$ kHz and $\tau \leq 135$ ms for satellite communications. It is highlighted that under the imperfect CSI scenario, the selected relay is not necessarily one having the best channel gain from the satellite. All imperfect CSI curves (red color) are plotted based on Monte-Carlo simulations, whereas the others (blue color) are plotted via Eq. (9). From Fig. 4, it is certain that the curves with perfect CSI outperform its counterpart. However, the harmful effect caused by the imperfect CSI can be significantly mitigated by increasing the number of relays. For example, the imperfect CSI with $N = 3$ is already better than the perfect

CSI with $N = 2$ for case $\Psi = \Phi = 15$ dB. This figure also reveals that scaling up N is monotonically decreasing the OP. Nevertheless, there exists a lower bound when increasing N. The main reason behind this phenomenon is that despite increasing N, of course, ameliorates the satellite-relay links, the e2e SINR is constrained by the second hop due to the limits of the partial relay selection scheme.

V. Conclusions

The performance of the STN was studied in the present paper under the impact of the CCI. Particularly, the outage probability was derived in a closed-form expression. Numerical results showed that both increasing the number of relays and the transmit power at S and R are beneficial for the OP. The paper can be extended in several directions. One of the possible extensions of the current work is to rigorously identify the impact of the large-scale path-loss [20]. Another possible extension is to apply reconfigurable intelligent surface (RIS) to further enhance the system performance [14].

Appendix

A. Proof of Theorem 1

In this section, we present the derivation of the CDF of the maximum of N i.i.d. squared Shadowed-Rician distribution. Let us first formulate the definition of the CDF as follows:

$$\begin{aligned}
F_Y(y) &= \Pr\left\{\max\left\{X_1,\ldots,X_N\right\} < y\right\} \\
&= \prod\nolimits_{n=1}^{N} \Pr\left\{X_n < y\right\} = \prod\nolimits_{n=1}^{N} F_{X_n}(y) \\
&\overset{(a)}{=} \prod_{n=1}^{N}\left[1 - \alpha_n \sum\nolimits_{k=0}^{m_n-1}\sum\nolimits_{p=0}^{k} \frac{(-1)^k (1-m_n)_k (\delta_n)^k}{k!p!(\beta_n-\delta_n)^{(k+1-p)}}\right. \\
&\left.\times x^p \exp\left(-\left(\beta_n-\delta_n\right)x\right)\right] \qquad (14) \\
&\overset{(b)}{=} \prod_{n=1}^{N}\left[1 + \sum_{n=1}^{N}((-1)^n/n!)\mathrm{T}\left(n,N,m,\alpha,\beta,\delta\right) x^{p_{\mathrm{S}}} \exp\left(-x v_{\mathrm{S}}\right)\right].
\end{aligned}$$

(a) is held by substituting the CDF of the Shadowed-Rician distribution in (2) and (b) is obtained by employing the following identity: $\prod_{n=1}^{N}(1-x_n) = 1 + \sum_{n=1}^{N}\frac{(-1)^n}{n!}\underbrace{\sum_{n_1=1}^{N}\cdots\sum_{n_n=1}^{N}}_{n_1\neq n_2\ldots\neq n_n}\prod_{t=1}^{n} x_{n_t}$. Finally by introducing the shorthand $\mathrm{T}\left(n,N,m,\alpha,\beta,\delta\right)$, v_{S}, and p_{S}, we obtain (7) and close the proof here.

B. Proof of Theorem 2

In this section, the CDF and PDF of the sum of N i.i.d. exponential RVs are given. Let us start with the moment generating function (MGF) of $Y = \sum_{n=1}^{N} X_n$ as follows:

$$\begin{aligned}
M_Y(s) &= \mathbb{E}\left\{\exp\left(-s\sum_{n=1}^{N} x_n\right)\right\} \\
&\overset{(a)}{=} \prod_{n=1}^{N}\left[\int_{x_n=0}^{\infty} \exp\left(-s x_n\right) f_{X_n}(x_n)\, dx_n\right] \\
&= \prod_{n=1}^{N} \lambda_n/(s+\lambda_n) \overset{(b)}{=} \lambda^N/(s+\lambda^N), \qquad (15)
\end{aligned}$$

where (a) is obtained due to the independent property of N RVs and (b) is held owing to the identical property. The PDF is then attained by employing the inverse Laplace transform as

$$\mathcal{L}^{-1}\left\{M_Y(s)\right\} = \frac{\lambda^N y^{N-1}\exp\left(-\lambda y\right)}{\Gamma(N)}, \qquad (16)$$

where $\mathcal{L}^{-1}\left\{.\right\}$ denotes as the inverse Laplace transform. The CDF is derived by taking the integration of the PDF and we finish the proof here.

$$F_Y(y) = \int_{t=0}^{y} \frac{\lambda^N t^{N-1}}{\Gamma(N)}\exp\left(-\lambda t\right) dt = \frac{\gamma\left(N,\lambda y\right)}{\Gamma(N)}. \qquad (17)$$

References

[1] X. Lin *et al.*, "5G from Space: An Overview of 3GPP Non-Terrestrial Networks," *IEEE Commun. Standards Mag.*, pp. 1–7, 2021.

[2] K. Guo *et al.*, "Performance Analysis of Hybrid Satellite-Terrestrial Cooperative Networks With Relay Selection," *IEEE Trans. Veh. Technol.*, vol. 69, no. 8, pp. 9053–9067, Aug. 2020.

[3] H. Kong *et al.*, "Multiuser scheduling for asymmetric FSO/RF links in satellite-UAV-terrestrial networks," *IEEE Wireless Commun. Lett.*, vol. 9, no. 8, pp. 1235–1239, 2020.

[4] ——, "Ergodic sum rate for uplink NOMA transmission in satellite-aerial-ground integrated networks," *Chinese J. of Aeronautics*, 2021.

[5] ——, "Performance analysis for rate splitting uplink NOMA transmission in high throughput satellite systems," *IEEE Wireless Commun. Lett.*, vol. 11, no. 4, pp. 816–820, 2022.

[6] L. Han *et al.*, "Outage Analysis of NOMA-Based Multiple-Antenna Hybrid Satellite-Terrestrial Relay Networks," *IEEE Commun. Lett.*, vol. 25, no. 4, pp. 1109–1113, Apr. 2021.

[7] P. K. Sharma *et al.*, "Performance analysis of overlay spectrum sharing in hybrid satellite-terrestrial systems with secondary network selection," *IEEE Trans. Wireless Commun.*, vol. 16, no. 10, pp. 6586–6601, 2017.

[8] H. Lin *et al.*, "Downlink outage analysis of integrated satellite-terrestrial relay network with relay selection and outdated CSI," in *IEEE VTC2021-Spring*, 2021, pp. 1–5.

[9] M. A. Vázquez *et al.*, "Precoding, scheduling, and link adaptation in mobile interactive multibeam satellite systems," *IEEE J. Sel. Areas Commun.*, vol. 36, no. 5, pp. 971–980, 2018.

[10] P. K. Upadhyay *et al.*, "Max-max user-relay selection scheme in multiuser and multirelay hybrid satellite-terrestrial relay systems," *IEEE Commun. Lett.*, vol. 20, no. 2, pp. 268–271, 2016.

[11] I. Krikidis *et al.*, "Amplify-and-forward with partial relay selection," *IEEE Commun. Lett.*, vol. 12, no. 4, pp. 235–237, Apr. 2008.

[12] ETSI, "Digital video broadcasting (dvb); system specifications for satellite services to handheld devices (sh) below 3 GHz, ts 102 585 v1.1.2," ETSI, Tech. Rep., Apr. 2008.

[13] V. Bankey *et al.*, "Ergodic capacity of multiuser hybrid satellite-terrestrial fixed-gain af relay networks with cci and outdated CSI," *IEEE Trans. on Veh. Technol.*, vol. 67, no. 5, pp. 4666–4671, 2018.

[14] T. V. Chien *et al.*, "Coverage probability and ergodic capacity of intelligent reflecting surface-enhanced communication systems," *IEEE Commun. Lett.*, vol. 25, no. 1, pp. 69–73, 2021.

[15] A. Jeffrey and D. Zwillinger, *Table of Integrals, Series, and Products - Eighth Edition*. Elsevier, 2014.

[16] G. Levin *et al.*, "Amplify-and-forward versus decode-and-forward relaying: Which is better?" 2012. [Online]. Available: https://www.site.uottawa.ca/∼sloyka/papers/2012/IZS-12_AF_vs_DF_27_12_11.pdf

[17] L. Yang *et al.*, "Performance analysis of amplify-and-forward hybrid satellite-terrestrial networks with cochannel interference," *IEEE Trans. Commun.*, vol. 63, no. 12, pp. 5052–5061, 2015.

[18] H. A. Suraweera *et al.*, "Capacity limits and performance analysis of cognitive radio with imperfect channel knowledge," *IEEE Trans. on Veh. Technol.*, vol. 59, no. 4, pp. 1811–1822, 2010.

[19] A. Guidotti *et al.*, "Architectures and key technical challenges for 5g systems incorporating satellites," *IEEE Trans. on Veh. Technol.*, vol. 68, no. 3, pp. 2624–2639, 2019.

[20] P. K. Sharma *et al.*, "Outage performance of multi-UAV relaying-based imperfect hardware hybrid satellite-terrestrial networks," *IEEE Systems J.*, pp. 1–4, 2021.